DOI 10.1007/s11237-015-9390-1
Theoretical and Experimental Chemistry, Vol. 50, No. 6, January, 2015 (Russian Original Vol. 50, No. 6, November-December, 2014)

OXYGEN REDUCTION NANOCOMPOSITE ELECTROCATALYSTS BASED ON POLYINDOLE, COBALT, AND ACETYLENE BLACK

Ya. I. Kurys, O. O. Ustavytska, D. O. Mazur, V. G. Koshechko, and V. D. Pokhodenko

UDC 541.64, 544.653, 546.73, 547.751

Polyindole (PIn), cobalt, and acetylene black (C) were used to obtain non-precious-metal nanocomposite electrocatalysts for the oxygen reduction reaction (ORR). We studied the composition, structure, and electrochemical properties of these materials. The PIn-Co/C_{pyr} obtained with treatment at elevated temperature, have much greater electrocatalytic activity in ORR in 0.05 M sulfuric acid in comparison with nonpyrolyzed (metal–polymer composite) PIn-Co/C, which may be attributed to differences in the catalytically-active sites in these composites.

Key words: *nanocomposite electrocatalysts, reduction of oxygen, polyindole, cobalt.*

Organic conducting polymers (CPs) such as polyaniline (PAn), polypyrrole (PPy), polythiophene, and polyphenylenevinylene and also composites based on such polymers are promising materials for molecular electronics, photovoltaics, chemical power sources, supercapacitors, chemosensors, and biosensors due to their set of attractive functional properties [1-3]. In particular, such materials are capable of acting as electrocatalysts for the oxygen reduction reaction (ORR) [3-8], which is a very important process in fuel cells. CPs themselves may demonstrate electrocatalytic properties in ORR [3, 4] and act as support matrices of catalytically-active compounds such as metal–phthalocyanine complexes, heteropolyacids, and platinum [2, 3, 5]. These materials may also act as cocatalysts for ORR in multicomponent hybrid nanocomposites, including nanocomposites containing platinum [6-8]. However, such CPs electrocatalysts are either expensive or display insufficient efficiency and/or instability in acid media, which hinders their industrial use.

In light of the high cost of platinum and the limited resources of this metal, workers have turned their attention to the development of electrocatalysts for ORR without noble metals but still displaying sufficient activity in this reaction. Among proposed systems to date, so-called Me-N-C catalysts (Me = metal) obtained by the joint pyrolysis of nitrogen-containing precursors, various cobalt and iron salts (or their combination), and carbon materials [9-11] should be allocated. The use of nitrogen-containing conjugated polymers such as PAn, PIn, and poly-*o*-phenylenediamine as nitrogen donors [9, 10, 12-15] leads to the formation of one of the most efficient Me-N-C catalysts, which has been considered as possible replacement for platinum [10]. Metal–polymer electrocatalysts based on nitrogen-containing CPs (PIn, PAn, and polyphenylenediamines), cobalt, and a carbon support have recently been proposed [12, 16-19]. These materials are mimetics of cobalt-containing porphyrins and have rather high activity in ORR even without heat treatment, which distinguishes them from other reported Me-N-C systems, as well as high stability upon use in acid electrolytes.

The use of nitrogen-containing CPs in the preparation of Me-N-C and metal–polymer electrocatalysts has been limited mainly to PPy or PAn. In particular, to our knowledge, there is no information in the literature on the use of polyindole (PIn) as

L. V. Pisarzhevskii Institute of Physical Chemistry, National Academy of Sciences of Ukraine, Prospekt Nauky, 31, Kyiv 03028, Ukraine. E-mail: kurys@inphyschem-nas.kiev.ua. Translated from Teoreticheskaya i Éksperimental'naya Khimiya, Vol. 50, No. 6, pp. 367-374, November-December, 2014. Original article submitted October 16, 2014.

a component of metal–polymer nanocomposite electrocatalysts for ORR or as a polymer nitrogen donor in the pyrolytic formation of Me-N-C electrocatalysts. On the other hand, PIn has high electrochemical stability and, in contrast, for example, to PAn, resistance to hydrolytic degradation [20]. Structural fragments of PIn, as in the case of PPy, are somewhat similar to porphyrins.

Hence, in this work, we attempted to obtain nonpyrolyzed (metal–polymer) and pyrolyzed (Me-N-C) nanocomposite electrocatalysts for ORR based on PIn, cobalt, and acetylene black and to study the effect of the preparation conditions (using or not using high temperature treatment and the type of precursors in carrying out the pyrolysis) on the composition, structure, and electrochemical properties of these materials.

EXPERIMENTAL

A sample of 99+% indole obtained from Acros Organics, highly-disperse 99+% acetylene carbon black with bulk density 80-120 g/L from Alfa Aesar, >98% $Co(NO_3)_2 \cdot 6H_2O$ from Aldrich, >97% $FeCl_3$ from Aldrich, >98% $NaBH_4$ from Aldrich, and >99.5% acetonitrile from Aldrich were used for preparation of the composites without further purification as well as aqueous solutions of NaOH and H_2SO_4.

The PIn-Co/C metal–polymer nanocomposite was synthesized by the oxidative polymerization of indole [20] in the presence of a dispersion of acetylene black with subsequent introduction of cobalt into the prepared polymer-modified carbon support (PIn/C) analogously to the approach presented by Bashyam and Zelenay [16]. A sample of 1.5 g acetylene black was dispersed in 150 mL acetonitrile. Then, 0.3 g (2.56 mmol) indole was dissolved in this dispersion. A solution of the oxidizing agent, namely, 1.25 g (7.68 mmol) $FeCl_3$ in 5 mL water, was added slowly dropwise with stirring to the resultant suspension. After 4 h, the polymerization was terminated. The PIn/C composite was filtered off, washed with acetonitrile, then water, and dried at 60 °C. A solution of 0.83 g $Co(NO_3)_2 \cdot 6H_2O$ in 8 mL water was added to a dispersion of 2 g PIn/C in 34 mL water in a three-necked flask. The temperature was brought to 75-80 °C and the suspension was stirred for 0.5 h. Then, a solution of 1.76 g $NaBH_4$ and 0.12 g NaOH in 168 mL water (pH 11-12) was added dropwise with stirring to the reaction mixture. The reduction of Co(II) ions in the composite was continued under these conditions, measuring the pH of the mixture every half hour; the pH gradually decreased. When the pH reached a constant value, the reaction mixture was cooled to room temperature. The precipitate of PIn-Co/C composite was filtered off and washed repeatedly with 0.05 M sulfuric acid and, then, water until the pH of the wash water was ~7. The product was then dried at 90 °C in a dry box.

In order to obtain the pyrolyzed PIn-Co/C_{pyr} nanocomposite, we used PIn-Co/C itself (PIn-Co/C_{pyr}**-1**), PIn/C impregnated with aqueous $Co(NO_3)_2 \cdot 6H_2O$ (10 mass % Co) (PIn-Co/C_{pyr}**-2**), and a mixture of PIn with acetylene black (1 : 5, mass %) homogenized by ultrasonic dispersion and impregnated with aqueous $Co(NO_3)_2 \cdot 6H_2O$ (10 mass % Co) (PIn-Co/C_{pyr}**-3**) as precursors. The heat treatment of the corresponding precursors was carried out in a tube furnace in an argon stream at 800 °C over 2 h. The heating rate was 5 °C/min. The pyrolyzed PIn-Co/C_{pyr} composites obtained were treated with 0.05 M sulfuric acid for 3 h with stirring, washed on a filter with water until the pH of the wash water was ~7, and dried at 90 °C in a dry box.

The morphology of the composites was studied using a Tescam Mira 3 LMU scanning electron microscope with secondary and backscattered electrons. The polymer content in the composites was evaluated by C,H,N analysis using a Carlo Erba instrument. A Thermoelectron SOLAAR S4 two-beam automatic atomic absorption spectrometer was used to determine the Co content in the composites. The samples were treated with concentrated sulfuric acid at 80-90 °C. The mixture was introduced into 2% nitric acid and filtered using the filtrate to determine cobalt, while the precipitate was checked to determine completion of the cobalt dissolution by X-ray fluorescence analysis on an Oxford Instruments X-Supreme 8000 spectrometer. The X-ray diffraction patterns of the composites were taken on a Bruker D8 ADVANCE diffractometer using filtered CuK_α radiation (λ = 0.154 nm). The IR spectra of the PIn sample tableted with KBr were taken on a Perkin Elmer SPECTRUM ONE Fourier Transform IR spectrometer.

The electrochemical studies of the nanocomposites obtained were carried out by cyclic voltammetry in an undivided cell. The working electrode was a glassy carbon disk with 0.03 cm^2 visible surface area. The auxiliary electrode was a platinum mesh and the reference electrode was Ag/AgCl (3.0 mol/L KCl), E = 0.202 V vs. standard hydrogen electrode using a computerized electrochemical unit containing a PI-50-1.1 potentiostat. The potential scan rate was 2 mV/s. The electrolyte was 0.05 M aqueous sulfuric acid. The nanocomposite was placed onto the surface of the electrode as a thin layer with Nafion. For

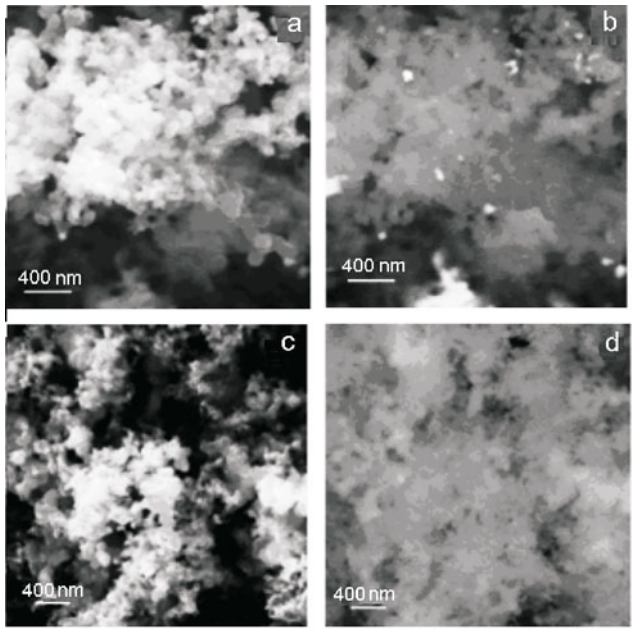

Fig. 1. SEM images of samples of PIn-Co/C (a, b) and PIn-Co/C_{pyr}**-1** (c, d) with secondary (a, c) and backscattered electrons (b, d).

this purpose, 2 mg nanocomposite and 8 μL 5% ethanolic Nafion (supplied by Aldrich) in 48 mL ethanol was ultrasonically dispersed. Then, 2 μL of the dispersion was placed onto the electrode with further drying in the air.

RESULTS AND DISCUSSION

Scanning electron microscopy was used to study the morphology of the PIn-Co/C metal–polymer composite before and after high-temperature treatment in an inert atmosphere (PIn-Co/C_{pyr}**-1**). Polymer-coated spherical particles of acetylene black (50-80 nm) predominate in the secondary electron microphotograph of PIn-Co/C (Fig. 1a). On the other hand, predominantly isolated light contrast nanoparticles attributed to the cobalt-containing phase are clearly seen between the dark contrast polymer–carbon nanoparticles in the image of the same segment taken with backscattered electrons due to the presence of light elements, namely, carbon and nitrogen, in their atomic composition (Fig. 1b).

The morphology of the pyrolyzed composite PIn-Co/C_{pyr}**-1** differs markedly from the morphology of PIn-Co/C already examined. Heat treatment of the sample leads to significant aggregation of the acetylene black granules (Fig. 1c) and disappearance of the light contrast particles in the backscattered electron microphotograph (Fig. 1d), which is in accord with the cobalt content in the metal–polymer and pyrolyzed polyindole nanocomposites.

The cobalt mass fraction in PIn-Co/C is 8 mass %, while in pyrolyzed composites PIn-Co/C_{pyr}**-1**, PIn-Co/C_{pyr}**-2**, and PIn-Co/C_{pyr}**-3** it does not exceed 0.1-0.3 mass %. The formation of a significant amount of metallic cobalt in the composites apparently occurs during the heat treatment. The metallic cobalt is then washed out of these samples using sulfuric acid after synthesis. The nitrogen contents in the unpyrolyzed and heat-treated composites according to the C,H,N-analysis also differ (1.4 and <0.1 mass %, respectively) since the decomposition of the polymer component and the resultant nitrogen-containing fragments may be removed both directly by a stream of inert gas in the heat treatment and after final washing of the pyrolyzed composite with 0.05 M sulfuric acid and water. The data obtained indicated that the content of PIn in the metal–polymer PIn-Co/C composite is 11.7 mass %.

The low content of polymer in the PIn-Co/C composite and the overlap of the IR bands characteristic for PIn and acetylene black did prevented the use of IR spectroscopy for an unequivocal interpretation of the structure of the polymer in the unpyrolyzed metal–polymer composite. With this in mind and also assuming that the molecular structure of PIn in the resultant

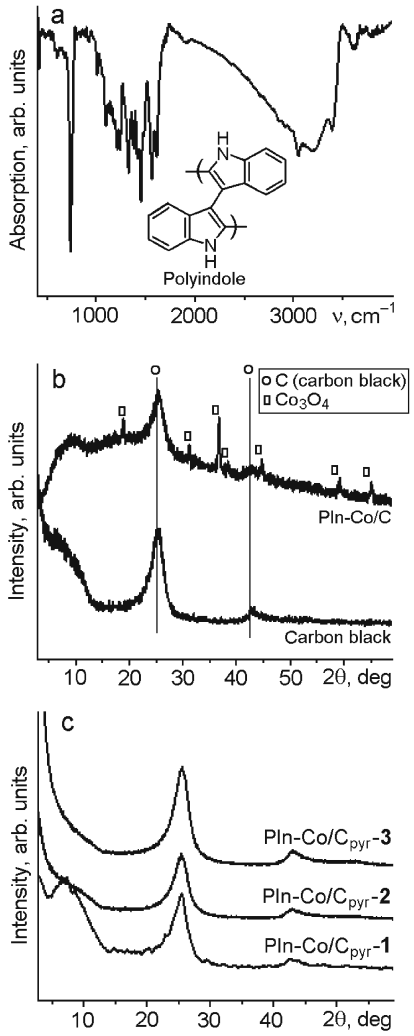

Fig. 2. IR spectrum of pure PIn (a) and X-ray diffraction patterns of the initial acetylene black and PIn-Co/C composite (b) as well as of the pyrolyzed composites PIn-Co/C_{pyr}-**1**, PIn-Co/C_{pyr}-**2**, and PIn-Co/C_{pyr}-**3** (c).

PIn-Co/C may be somewhat similar to the pure polymer, we studied the IR spectra of PIn synthesized analogously to the corresponding composite. The spectrum shown in Fig. 2a shows bands characteristic for PIn at 3398 (ν_{N-H}) and 1567 cm^{-1} (δ_{N-H}) [21, 22]. The finding of these bands in the IR spectrum indicates that the unsaturated nitrogen atom of the monomer is not involved in the polymerization and, thus, may participate in the formation of C/CoN_x sites in the PIn-Co/C composite, on which, according to various workers [9-11], the adsorption, activation, and catalytic transformation of O_2 occur. On the other hand, the finding of strong IR bands for the polymer related to stretching (1456 cm^{-1}) and out-of-plane deformation vibrations (741 cm^{-1}) of C—H bonds in aromatic ring as well as the absence of bands at 721 and 767 cm^{-1} observable for the monomer (δ_{C-H} for C-2 and C-3 of the indole molecular, respectively [21]) indicate that the polymerization of indole proceeds mainly through the C-2 and C-3 carbon atoms of the monomer pyrrole ring [21-23]. The spectrum of the prepared polymer also has a series of other bands characteristic for PIn at 1616, 1486, 1423, 1383, 1332, 1217, and 1106 cm^{-1}. Detailed interpretations of the bands have been given by various workers [21-23]. We should also note the presence of a broad

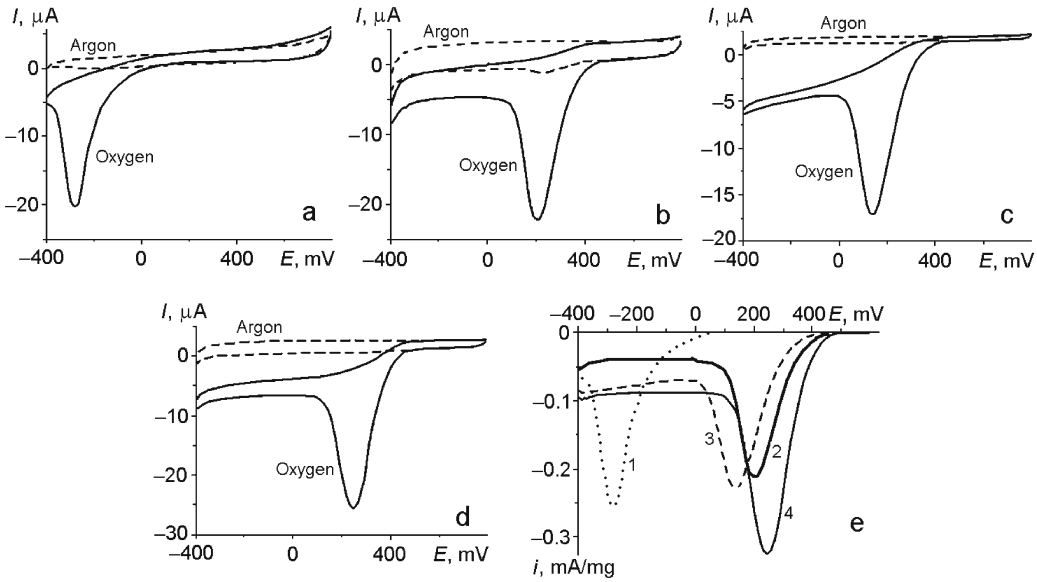

Fig. 3. Cyclic voltammograms (a-d) and curves for the electrocatalytic reduction of oxygen obtained in 0.05 M H_2SO_4 for a vitreous carbon electrode modified by a catalytic layer of PIn-Co/C (a, e, 1), PIN-Co/C_{pyr}-**1** (b, e, 2), PIn-Co/C_{pyr}-**2** (c, e, 3), and PIn-Co/C_{pyr}-**3** (d, e, 4).

IR band for PIn at ~3600 cm^{-1} (ν_{O-H}), which is probably due to the presence of water adsorbed by the polymer not completely removed during the drying process.

Figure 2b gives the X-ray diffraction patterns of the initial acetylene black and the unpyrolyzed PIn-Co/C composite. The diffraction pattern of acetylene black has reflections at 2θ = 25.4° and 42.9°, which correspond to the C(002) and C(100) crystal planes [24] and indicate a significant contribution of a graphite-like phase, and a broad halo in the small-angle region. In addition to reflections related to the carbon composite, the X-ray diffraction pattern of the PIn-Co/C composite shown in Fig. 2b has broad bands characteristic for PIn [23] with maxima at 2θ ≈ 18° and 25°, indicating a predominantly amorphous state of the polymer in the composite. Furthermore, the diffraction pattern of the composite has a series of pronounced reflections (2θ = 18.9°, 31.1°, 36.7°, 38.5°, 44.7°, 59.3°, and 65.1°), which may be assigned to the Co_3O_4 phase [25, 26], apparently formed as shells on the metallic cobalt nanoparticles during preparation of the composite [18]. Considering also that the macromolecules may hinder crystallization of the cobalt-containing particles [27], we cannot exclude that a portion of the cobalt in the Co^{δ} state ($0 < \delta \leq 2^{+}$) may exist in PIn-Co/C as an amorphous form not seen in the diffraction pattern and also coordinate to the polymer chain nitrogen atoms [16].

The diffraction patterns of the pyrolyzed nanocomposites PIn-Co/C_{pyr}-**1**, PIn-Co/C_{pyr}-**2**, and PIn-Co/C_{pyr}-**3** (Fig. 2c) are similar to each other but differ significantly from the pattern for the metal–polymer composite PIn-Co/C. The complete or virtually complete predominance of reflections related to the carbon support in the diffraction patterns of the pyrolyzed samples is in accord with the SEM results and with the composition established for these materials.

The significant differences in the structure of the nanocomposites related to employing or not employing high-temperature heat treatment during preparation and differences in the precursors used in the preparation of the pyrolyzed nanocomposites PIn-Co/C_{pyr}-**1**, PIn-Co/C_{pyr}-**2**, and PIn-Co/C_{pyr}-**3** may also lead to differences in the redox properties of these materials, particularly in the oxygen reduction reaction (ORR). In order to check this hypothesis using cyclic voltammetry, we studied the electrochemical properties of these nanocomposites in deaerated and oxygen-saturated solutions of 0.05 M sulfuric acid. The capacity of these nanocomposites to act as electrocatalysts for ORR and their activity were characterized by the electrocatalytic oxygen reduction curves, which show the difference between the cathodic branches of the cyclic voltammograms (CVs) taken with and without oxygen in the electrolyte.

TABLE 1. Catalytic Current Onset Potentials (E_{onset}), Catalytic Current Maxima (E_{max}) and Catalytic Current (i) for Nanocomposite Electrocatalysts for ORR Based on PIn

Electrocatalyst	E_{onset}, mV	E_{max}, mV	i, mA/mg
PIn-Co/C	0	–280	0.25
PIn-Co/C_{pyr}-**1**	430	200	0.21
PIn-Co/C_{pyr}-**2**	440	140	0.23
PIn-Co/C_{pyr}-**3**	470	250	0.33

These studies showed that the unmodified glassy carbon (GC) electrode does not display significant electrocatalytic activity in ORR under the measurement conditions. On the other hand, an irreversible peak arises in the oxygen-saturated electrolyte on the cathodic branches of the CVs of glassy carbon electrodes modified by all the composites obtained (Fig. 3), indicating that these electrodes are active in this reaction. Figure 3 and Table 1 show that the functional characteristics of these electrocatalysts depend on whether or not these materials are subjected to heat treatment during preparation and, in the case of the composites obtained by pyrolysis, on the nature of the initial precursors.

As an electrocatalyst for ORR, the metal–polymer nanocomposite PIn-Co/C has low potentials for the appearance of a catalytic current (E_{onset}) and a low catalytic current maximum (E_{max}) (Table 1, Fig. 3a,e), which are inferior to the values for the analogous nanocomposites based on PPy, PAn, and polyphenylenediamines [16-19] but exceed those values found in our work for pure acetylene black, PIn, and PIn/C not containing cobalt. As noted above, the rather high activity of the metal–polymer electrocatalysts based on nitrogen-containing organic conducting polymers and cobalt is attributed to catalytically-active C/CoN_x or CoN_x sites [9, 10, 16-19]. Not excluding that such sites may also be formed during the preparation of PIn-Co/C, we may conclude that, as a minimum, some of the cobalt "captured" in the composite is present as Co_3O_4 as indicated by the diffraction pattern of this composite (Fig. 2b). Apparently, the smaller amount of C/CoN_x or CoN_x sites in PIn-Co/C in comparison with analogs based on PAn or PPy (due to the presence of Co_3O_4 with only slight activity in ORR in acid electrolytes) may be one of the reasons for the observed poor functional characteristics of this catalyst.

Heat treatment of PIn-Co/C in an inert atmosphere leads to PIn-Co/C_{pyr}-**1** with significantly enhanced activity in ORR (Fig. 3b,e, Table 1) in comparison with the unpyrolyzed composite, which is seen in the anodic shift of E_{onset} and E_{max} in the CVs by ~430 and 480 mV, respectively.

It was of interest to clarify how the type of precursors used in the pyrolysis preparation of the PIn nanocomposite electrocatalysts affects the activity in ORR of such heat-treated composites. Our studies (Fig. 2b-e, Table 1) showed that there are no significant differences in the functional characteristics of PIn-Co/C_{pyr}-**1**, PIn-Co/C_{pyr}-**2**, and PIn-Co/C_{pyr}-**3**. However, a slight anodic shift of E_{onset} is observed in the series PIn-Co/C_{pyr}-**1** < PIn-Co/C_{pyr}-**2** < PIn-Co/C_{pyr}-**3**, while the largest E_{max} (Table 1) is found for composite PIn-Co/C_{pyr}-**3** obtained in the combined pyrolysis of acetylene black, PIn, and $Co(NO_3)_2 \cdot 6H_2O$. The observed differences in the electrocatalytic properties of the pyrolyzed composites may be related to slight differences in the content of PIn and cobalt (directly participating in formation of the catalytically-active sites) in the precursors used in the preparation of these electrocatalysts. The PIn : Co ratio (mass %) prior to the heat treatment of the precursors was 11.7 : 8 in the synthesis of PIn-Co/C_{pyr}-**1**, 11.7 :1 0 for PIn-Co/C_{pyr}-**2**, and 15 : 10 for PIn-Co/C_{pyr}-**3**.

We should note that, despite the almost complete absence of cobalt in the pyrolyzed electrocatalysts, the activity in ORR in all cases is much greater than the activity found for unpyrolyzed PIn-Co/C. This discrepancy may be attributed to differences in the nature of the catalytically-active sites in these samples. The results of Wu [14] and Wang [15] permit us to propose that C/N_x sites are responsible for activity in ORR in nanocomposite PIn-Co/C_{pyr} electrocatalysts rather than C/CoN_x or CoN_x sites.

Thus, we have obtained nanocomposite electrocatalysts not containing noble metals, namely, metal–polymer (PIn-Co/C) and pyrolyzed Me-N-C composites (PIn-Co/C_{pyr}) based on polyindole, cobalt, and acetylene black. The heat treatment step in the preparation of PIn-Co/C_{pyr} leads to a significant increase in activity of the catalysts in ORR in an acid electrolyte (E_{onset} to 670 mV and E_{max} to 450 mV vs. standard hydrogen electrode) in comparison with the unpyrolyzed analog. The observed differences in the electrocatalytic activity of PIn-Co/C and PIn-Co/C_{pyr} may be related to differences in the nature of the catalytically-active sites in the composites (absence or presence of cobalt), on which the activation and catalytic transformations of oxygen take place.

This work was carried out with the partial financial support of the State Science and Technology Program "Nanotechnology and nanomaterials" (Project No. 6.22.3.11) and the Joint Integrated Basic Research Program of the National Academy of Sciences of Ukraine "Hydrogen in alternative energy and new technologies" (Project No. 6-14).

REFERENCES

1. A. G. MacDiarmid, *Angew. Chem. Int. Ed.*, **40**, No. 14, 2581-2590 (2001).
2. A. Malinauskas, J. Malinauskiene, and A. Ramanavičius, *Nanotechnology*, **16**, No. 1, R51-R62 (2005).
3. B. I. Podlovchenko and V. N. Andreev, *Usp. Khim.*, **71**, No. 10, 950-965 (2002).
4. V. G. Khomenko, V. Z. Barsukov, and A. S. Katashinskii, *Electrochim. Acta*, **50**, Nos. 7/8, 1675-1683 (2001).
5. Z. Qi and P. G. Pickup, *Chem. Commun.*, No. 21, 2299-2300 (1998).
6. O. Yu. Posudievsky, Ya. I. Kurys, and V. D. Pokhodenko, *Synth. Met.*, **144**, No. 2, 107-111 (2004).
7. Ya. I. Kurys', N. S. Netyaga, V. G. Koshechko, and V. D. Pokhodenko, *Teor. Éksp. Khim.*, **43**, No. 5, 307-314 (2007). [*Theor. Exp. Chem.*, **43**, No. 5, 334-342 (2007) (English translation).]
8. Ya. I. Kurys, E. S. Dodon, E. A. Ustavitskaya, et al., *Élektrokhimiya*, **48**, No. 11, 1161-1168 (2012).
9. F. Jaouen, E. Proietti, M. Lefevre, et al., *Energy Environ. Sci.*, **4**, No. 114, 114-130 (2011).
10. Z. Chen, D. Higgins, A. Yu, et al., *Energy Environ. Sci.*, **4**, No. 9, 3167-3192 (2011).
11. A. Garsuch, A. Bonakdarpour, G. Liu, et al., *Handbook of Fuel Cells: Advances in Electrocatalysis, Materials, Diagnostics and Durability*, W. Vielstrich, H. A. Gasteiger, and H. Yokokawa (eds.), Vols. 5, 6, John Wiley & Sons, Weinheim (2009), p. 71.
12. K. Lee, L. Zhang, H. Lui, et al, *Electrochim. Acta*, **54**, No. 20, 4704-4711 (2009).
13. M. Lefevre, E. Proietti, F. Jaouen, and J. P. Dodelet, *Science*, **324**, No. 5923, 71-74 (2009).
14. G. Wu, K. L. More, C. M. Johnston, and P. Zelenay, *Science*, **332**, No. 6028, 443-447 (2011).
15. P. Wang, Z. Ma, Z. Zhao, and L. Jia, *J. Electroanal. Chem.*, **611**, Nos. 1/2, 87-95 (2007).
16. R. Bashyam and P. Zelenay, *Nature Lett.*, **443**, No. 7, 63-66 (2006).
17. C. M. Johnston, P. Piela, and P. Zelenay, *Handbook of Fuel Cells: Advances in Electrocatalysis, Materials, Diagnostics and Durability*, W. Vielstich, H. A. Gasteiger, and H. Yokokawa (eds.),Vols. 5, 6, John Wiley & Sons, Weinheim (2009), p. 48.
18. Z. Yin, T. Hu, J. Wang, et al., *Electrochim. Acta*, **119**, 144-154 (2014).
19. Ya. I. Kurys, O. O. Ustavytska, V. G. Koshechko, and V. D. Pokhodenko, *Electrocatalysis*, **6**, No. 1, 117-125 (2015).
20. G. Rajasudha, D. Rajeswari, B. Lavanya, et al., *Colloid Polym. Sci.*, **283**, No. 5, 575-582 (2005).
21. H. Talbi, J. Ghanbaja, D. Billaud, and B. Humbert, *Polymer*, **38**, No. 9, 2099-2106 (1997).
22. J. Xu, J. Hou, W. Zhou, et al., *Spectrochim. Acta A*, **63**, No. 9, 723-728 (2006).
23. N. B. Taylan, B. Sari, and H. I. Unal, *J. Polym. Sci. B*, **48**, No. 12, 1290-1298 (2010).
24. B. Manoj and A. G. Kunjomana, *Int. J. Electrochem. Sci.*, **7**, No. 4, 3127-3134 (2012).
25. X. Liu and C. T. Prewitt, *Phys. Chem. Miner.*, **17**, No. 2, 168-172 (1990).
26. W. L. Smith and A. D. Hobson, *Acta Crystallogr. B*, **29**, No. 2, 362-363 (1973).
27. J. Wang, H. Qin, J. Liu, et al., *J. Phys. Chem. C*, **116**, No. 38, 20225-20229 (2012).